Inorg. Chem. **2007**, *46*, 4868–4875

A Structural and Theoretical Investigation of Equatorial cis and trans Uranyl Phosphinimine and Uranyl Phosphine Oxide Complexes $UO_2Cl_2(Cy_3PNH)_2$ and $UO_2Cl_2(Cy_3PO)_2$

L. Jonas L Häller,[†] Nikolas Kaltsoyannis,*[,†] Mark J. Sarsfield,*[,‡] Iain May,*[,§] Stéphanie M. Cornet,[||] Michael P. Redmond,[||] and Madeleine Helliwell[⊥]

Department of Chemistry, University College London, 20 Gordon Street, London WC1H, U.K., Nexia Solutions, British Technology Centre, Sellafield, Seascale, Cumbria CA20 1PG, U.K., Inorganic, Isotope and Actinide Chemistry (C-IIAC), Los Alamos National Laboratory, Mail Stop J-514, Los Alamos, New Mexico 87545, Centre for Radiochemistry Research, School of Chemistry, The University of Manchester, Manchester M13 9PL, U.K., and School of Chemistry, The University of Manchester, Manchester M13 9PL, U.K.

Received October 23, 2006

Phosphinimine ligands (Cy_3PNH) readily react with $UO_2Cl_2(THF)_3$ (THF = tetrahydrofuran) to give $UO_2Cl_2(Cy_3PNH)_2$, which contains strong U–N interactions and exists as cis and trans isomers in the solid and solution state. Solution NMR experiments and computational analysis both support the trans form as the major isomer in solution, although the cis isomer becomes more stabilized with an increase in the dielectric constant of the solvent. Mayer bond orders, energy decomposition analysis, and examination of the molecular orbitals and total electron densities support a more covalent bonding interaction in the U–$NHPCy_3$ bond compared with the analogous bond of the related U–$OPCy_3$ compounds.

Introduction

In 1935, Fankuchen first suggested that the uranyl $[UO_2]^{2+}$ unit contained a linear dioxo arrangement,[1] a generic structural motif for actinyl complexes later confirmed by Zachariasen[2−4] and others. Perpendicular to the dioxo group, the remaining equatorial coordination sites can be filled by three, four, five, or six donor atoms. Due to its interesting chemical properties, industrial/environmental relevance, comparative ease of chemical manipulation (stable oxidation state and low radioactivity), and relative ease of computational study (f^0), the uranyl cation is the most commonly studied actinide species. Examples of current progress in uranyl chemistry can be found in a recent review article.[5]

The number of donor atoms in the equatorial plane is generally determined by the steric and electronic properties of the ligands. Pentagonal-bipyramidal geometry is by far the most common arrangement; however, more sterically demanding ligands (such has the heavier halides) tend to induce tetragonal-bipyramidal (TB) structures. A growing family of complexes with TB geometry of the type $AnO_2X_2L_2$ (e.g., X = Cl, Br, I, NCO; L = OPR_3, $OAsR_3$, H_2O)[6−10] can potentially exist as cis (**I**) or trans (**II**) isomers. Given the

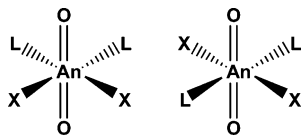

I **II**

steric constraints that lead to a TB geometry, it might be expected that the trans form would be the more stable. This has been noted in a few reports,[6−7] but no detailed study of the isomerism has been presented.

* To whom correspondence should be addressed. E-mail: n.kaltsoyannis@ucl.ac.uk (N.K.), mark.sarsfield@nexiasolutions.com (M.J.S.), iainmay@lanl.gov (I.M.).
† University College London.
‡ Nexia Solutions.
§ Los Alamos National Laboratory.
|| Centre for Radiochemistry Research, The University of Manchester.
⊥ School of Chemistry, The University of Manchester.

(1) Fankuchen, I. *Z. Kristallogr.* **1935**, *91*, 473.
(2) Zachariasen, W. H. *Acta Crystallogr.* **1948**, *1*, 281.
(3) Zachariasen, W. H. *Acta Crystallogr.* **1954**, *7*, 788.
(4) Zachariasen, W. H. *Acta Crystallogr.* **1954**, *7*, 795.
(5) Ephritikhine, M. *Dalton Trans.* **2006**, 2501.
(6) Akona, J.; Fawcett, J.; Holloway, J. H.; Russell, D. R. *Acta Crystallogr., Sect. C: Cryst. Struct. Commun.* **1991**, *47*, 45.

10.1021/ic062031m CCC: $37.00
Published on Web 05/17/2007

We recently reported the formation of uranyl phosphinimine complexes $UO_2Cl_2(R_3PNH)_2$ (R = Ph, Cy). These complexes are structurally very similar to the phosphine oxide ($UO_2Cl_2(R_3P{=}O)_2$) analogues with a linear axial dioxo uranium unit surrounded by two chloro units and two phosphinimines in the equatorial plane, providing overall TB geometry. It is possible that the equatorial ligands may be arranged cis or trans to each other, and evidence for this was found by NMR spectroscopy in solution, although only the trans isomer of $UO_2Cl_2(Ph_3PNH)_2$ was structurally characterized.[11]

We also demonstrated a distinct preference for U−$NHPR_3$ vs U−OPR_3 bonding when it might be expected that the harder oxygen donor would bind preferentially (see Scheme 1). Solutions of $UO_2Cl_2(Cy_3PNH)_2$ do not react with Cy_3PO even in an excess of the latter or at elevated temperature (40 °C). In contrast, adding 2 equiv of Cy_3PNH to $UO_2Cl_2(Cy_3PO)_2$ results in the immediate displacement of the Cy_3PO ligand and the quantitative formation of $UO_2Cl_2(Cy_3PNH)_2$.[11] These observations, together with the relatively large change in the N*H* chemical shift upon complexation of the R_3PNH ligand ($\Delta\delta$ ca. 6 ppm) and the unusually short U−N bond lengths, implied that a covalent contribution to the bonding may be responsible, which warranted further investigation. However, this can be difficult to probe using only structural and spectroscopic techniques.

Here, we report the isolation and structural characterization of both cis and trans isomers of $UO_2Cl_2(Cy_3PNH)_2$ (**1**) and the trans isomer of $UO_2Cl_2(Cy_3PO)_2$ (**2**), the results of further NMR experiments probing solution speciation, and provide molecular orbital calculations at the DFT level to help explain many of the above observations. We regarded this as an excellent opportunity to test current computational methodology on a well-defined and interesting actinyl system.

Experimental and Computational Details

General Experimental. The ligand precursor Cy_3P (Strem), was used as received. Cy_3PNH was prepared using literature methods.[12−13] All reactions and manipulations were performed under argon using standard Schlenk techniques or an inert atmosphere drybox. The solvents were purified by distillation from sodium (toluene), sodium/benzophenone ketyl (THF) (THF = tetrahydrofuran), and P_2O_5 (CH_2Cl_2) and stored over molecular sieves (4 Å) in a drybox. ^1H, $^{13}C\{^1H\}$, and $^{31}P\{^1H\}$ NMR spectra were recorded on a Bruker Avance 400 instrument at 400, 100, 376, and 162 MHz, respectively. Raman and UV−vis spectroscopy data were recorded on Bruker Equinox 55 FTIR/Raman (Nd:YAG 1064 nm) and Varian Cary 500 instruments, respectively. Elemental analysis was performed on a Carlo ERBA Instruments CHNS-O EA1108 elemental analyzer for C, H, and N and by a Fisons Horizon elemental analysis ICP-OED spectrometer for U and P. The X-ray diffraction study for all compounds was carried out on a Bruker AXS SMART diffractometer. Data collection and structure refinement was achieved using standard Bruker AXS control and integration software and *SHELXTL* for all compounds.

Scheme 1. A Comparison of the Ligand-Substituting Ability of Cy_3PO and Cy_3PNH

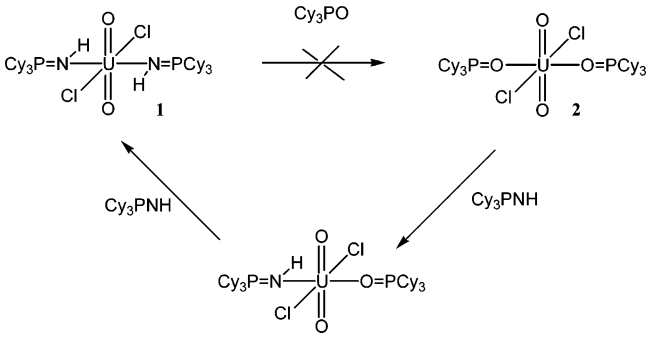

Caution! *In addition to the radioactive hazards associated with ^{238}U, this metal is toxic and should only be handled in an appropriate radiochemistry laboratory following approved procedures.*

Synthesis and Characterization of $UO_2Cl_2(Cy_3PNH)_2{\cdot}2CH_2Cl_2$ (1) and $UO_2Cl_2(Cy_3PO)_2{\cdot}2CH_2Cl_2$ (2). The synthetic procedures for **1** and **2** were essentially the same; thus, only those of **1** will be discussed in detail. A solution of $UO_2Cl_2THF_3$ (0.50 g, 1.03 mmol) in THF (20 cm^3) was treated with 2 equiv of Ph_3PNH (0.57 g, 2.06 mmol) dissolved in THF. The reaction was stirred for 1 h while a pale yellow precipitate developed. The solution was filtered, and the solid obtained was washed with THF and hexane (10 cm^3 × 2) and dried under vacuum. Layering a dichloromethane solution of **1** with hexane and storing at −15 °C overnight gave yellow cubic crystals of the trans isomer, whereas concentrated solutions of dichloromethane left at ambient temperature provided yellow rectangular blocks of the cis isomer. Crystals of *trans*-**2** were prepared by layering hexane over a saturated solution of **2** in dichloromethane.

$UO_2Cl_2(Cy_3PNH)_2{\cdot}2CH_2Cl_2$ (1·2CH_2Cl_2). Yield: 78% (cis/trans isomer ratio is ca. 1:9). Anal. Calcd for $C_{38}H_{72}Cl_6N_2P_2O_2U$: C, 41.43; H, 6.59; Cl, 19.31; N, 2.54; P, 5.62; U, 21.61. Found: trans C, 41.50; H, 6.71; Cl, 18.77; N, 2.49; P, 5.65; U, 21.37; cis C, 41.36; H, 6.93; Cl, 18.95; N, 2.57; P, 5.62; U, 21.55. IR, trans (4000−600 cm^{-1}, solid sample on ATR cell): 3345(w), 2932(s), 2851(s), 1542(w), 1444(m), 1355(m), 1322(w), 1297(w), 1278(w), 1218(w), 1180(w), 1169(w), 1109(m), 1075(m), 1065(w), 1024(s), 947(s), 913(w), 900(s), 852(m), 824(w), 757(w), 705(w); Raman (solid in glass capillary, 1600−600 cm^{-1}) 1444(m), 1353(w), 1296(m), 1285(w), 1273(w), 1202(w), 1047(w), 1030(m), 968(w), 851(w), 817(s, O=U=O_{symm}), 714(w), 700(m). IR, cis (4000−600 cm^{-1}, solid sample on ATR cell): 3340(w), 2930(s), 2853(s), 1445(m), 1269(w), 1229(w), 1178(w), 1118(w), 1105(w), 1006(m), 947(s), 892(s), 853(m), 817(m), 729(m), 699(m); Raman (solid in glass capillary, 1600−600 cm^{-1}) 1544(w), 1442(m), 1294(w), 1281(w), 1066(m), 1027(m), 970(w), 848(w), 822(s, O=U=O_{symm}) 704(m), 631(w). ^1H NMR (400 MHz, CD_2Cl_2, 0 °C): (2 N*HP*Cy_3 signals due to isomers) δ 1.20−2.40 (m, 66H, Cy), 5.56 (minor isomer; d, 0.1 H, Cy_3PNH, J_{HP} = 8.1 Hz), 5.82 (major isomer; d, 0.9 H, Cy_3PNH, J_{HP} = 7.8 Hz). $^{13}C\{^1H\}$ NMR (100 MHz, CD_2Cl_2, 0 °C, major isomer only): δ 26.1 (s, *p*-Cy), 26.8 (d, *m*-Cy, $^3J_{CP}$ = 2.8

(7) Arnáiz, F. J.; Miranda, M. J.; Aguado, R.; Mahía, J.; Maestro, M. A. *Polyhedron* **2001**, *20*, 3295.
(8) Bombieri, G.; Forsellini, E.; Day, J. P.; Azeez, W. I. *Dalton Trans.* **1978**, 677.
(9) Bombieri, G.; Forsellini, E.; Paoli, G. D.; Brown, D.; Tso, T.; Chung, J. *Dalton Trans.* **1979**, 2042.
(10) Crawford, M.-J.; Mayer, P.; Nöth, H.; Suter, M. *Inorg. Chem.* **2004**, *43*, *6860.*
(11) Sarsfield, M. J.; May, I.; Cornet, S. M.; Helliwell, M. *Inorg. Chem.* **2005**, *44*, *7310.*
(12) Dehnicke, K.; Kreiger, M.; Massa, W. *Coord. Chem. Rev.* **1999**, *182*, 19.
(13) Dehnicke, K.; Weller, F. *Coord. Chem. Rev.* **1997**, *158*, 103.

Hz), 27.3 (d, *o*-Cy, $^2J_{CP}$ = 7.3 Hz), 35.3 (d, *i*-Cy, $^1J_{CP}$ = 54.2 Hz). $^{31}P\{^1H\}$ NMR (162 MHz, CD_2Cl_2, 0 °C, 85% H_3PO_4): (two isomer signals relative intensities in parentheses) δ 58.1 (0.88), 58.8 (0.12).

$UO_2Cl_2(Cy_3PO)_2 \cdot 2CH_2Cl_2$ ($2 \cdot 2CH_2Cl_2$). Yield: 81%. Anal. Calcd for $C_{38}H_{70}Cl_6P_2O_4U$: C, 46.31; H, 7.12; Cl, 7.59; P, 6.65; U, 25.49. Found: C, 47.08; H, 7.52; Cl, 7.84; P, 6.65; U, 24.98. IR (4000−600 cm^{-1}, solid sample on ATR cell): 2923(m), 2849(m), 1444(m), 1360(w), 1327(w), 1298(w), 1212(w), 1171(w), 1116(m), 1083(sh), 1063(s), 995(m), 818(s), 889(m), 858(w), 824(w), 789(w), 764(w), 749(w), 715(w), 544(m), 530(m); Raman (3500−400 cm^{-1}, solid in glass capillary) 2989(w), 2941(vs), 2855(vs), 1447(m), 1353(w), 1294(w), 1118(w), 1097(w), 1029(m), 832(s, O═U═O_{symm}), 715(w), 699(w). ^1H NMR (400 MHz, CD_2Cl_2, 0 °C): δ 1.20−2.50 (m, 66H, Cy). $^{13}C\{^1H\}$ NMR (100 MHz, CD_2Cl_2, 0 °C): δ 26.2 (s, m, *p*-Cy), 27.1 (d, *o*-Cy, $^2J_{CP}$ = 12 Hz), 35.4 (d, *i*-Cy, $^1J_{CP}$ = 59 Hz). $^{31}P\{^1H\}$ NMR (162 MHz, CD_2Cl_2, 0 °C, 85% H_3PO_4): (two isomer signals relative intensities in parentheses) δ 73.4 (0.93), 73.0 (0.07).

Computational Details. DFT calculations were performed using the *Amsterdam Density Functional*[14] (ADF) quantum chemistry package with the PBE[15−16] generalized-gradient approximation exchange-correlation functional. TZP zero-order regular approximation (ZORA) all-electron basis sets were used on all atoms except C and H, where DZP ZORA all-electron basis sets were used. Isotropic shielding constants and chemical shifts were computed using the ADF NMR property program.[17−18] Relativistic effects were accounted for by the ZORA model, including scalar terms in all calculations and spin−orbit coupling in the NMR calculations (and as the total bond energies, dipole moments, and Hirshfeld charges are taken from the NMR calculations, spin−orbit coupling is included in the determination of those properties). The ADF NMR property program calculations employed all relativistic terms available, i.e., the mass-velocity, Darwin, and spin-Zeeman terms. The integration grid parameter was set to 5, the SCF convergence criterion was 10^{-7}, and the geometry convergence was 10^{-3} au $Å^{-1}$. Mayer bond orders[19] (MBOs) and Hirshfeld[20] charges were calculated at the optimized structures. Solvent effects were included by the conductor-like screening model[21−22] with the following values for the atomic radii: U = 2.0 Å, O = 1.6 Å, Cl = 1.8 Å, N = 1.6 Å, P = 2.0 Å, C = 1.8 Å, and H = 1.2 Å. The following solvent radii and dielectric constants were used : $CHCl_3$, r = 2.48 Å, ϵ = 4.9; CH_2Cl_2, r = 2.27 Å, ϵ = 8.93; CH_3Cl, r = 2.00, ϵ = 12.9; THF, r = 2.56 Å, ϵ = 7.58; H_2O, r = 1.385 Å, ϵ = 78.39. The orbital and total electron-density plots were generated using the *MOLEKEL* code.

ADF defines the molecular interaction energy as the energy difference between the molecular fragments in their final positions and at infinite separation. These molecular fragments may be individual atoms or groups of atoms, and for a discussion of the use of fragments within ADF, the reader is directed to a previous detailed description.[23] These fragments are placed at their positions within the molecule. At this point, there is an electrostatic interaction between them, comprising the nucleus−nucleus, nucleus−electron, and electron−electron Coulombic interactions. This electrostatic interaction is computed from the unperturbed and superimposed charge densities of the separate fragments. Next, it is ensured that the overall molecular wavefunction satisfies the Pauli principle. This is done by requiring that the one-electron orbitals of the combined fragments form a correct single-determinantal wavefunction. It is extremely unlikely, however, that this will be the case for the fragment orbitals when the fragments are simply placed at their positions within the molecule because the orbitals on the different fragments will not be orthogonal to one another. Thus, the next step is to orthogonalize the occupied fragment orbitals to obtain a correct single-determinantal, antisymmetrized molecular wavefunction. This will result in a change in the molecular charge density, and the accompanying energy change is known as the Pauli or exchange repulsion. The final part of the process is to allow the fragment orbitals to relax to self-consistency, and the interaction energy between the orbitals of the various fragments is defined as the electronic (or orbital) interaction.[24−25]

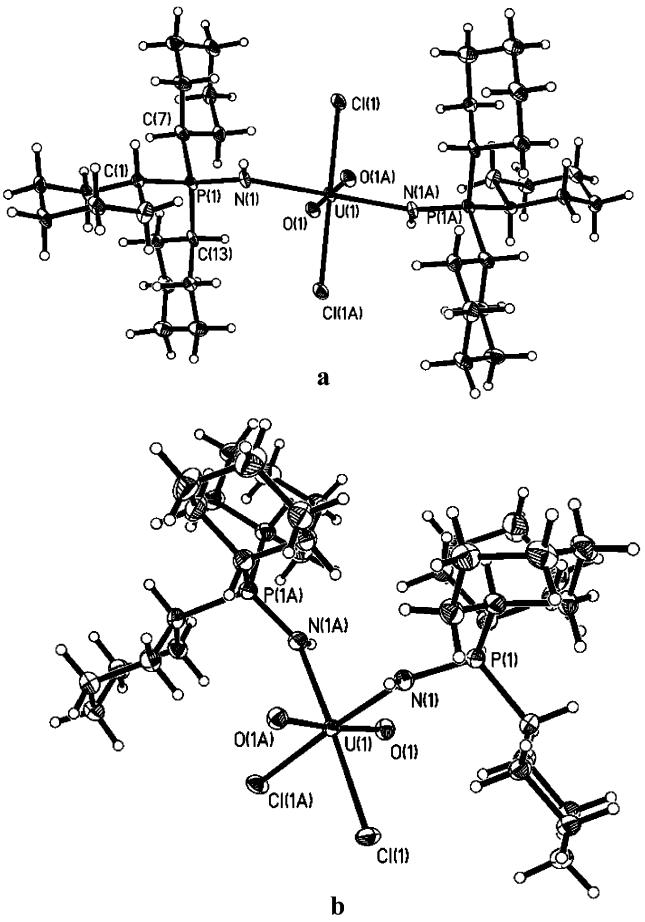

Figure 1. *ORTEP* representations of (a) $\mathbf{1}_{trans}$ and (b) $\mathbf{1}_{cis}$.

Experimental Results and Discussion

Structural Studies. *cis*- and *trans*-$UO_2Cl_2(Cy_3PNH)_2$ (1). Both *cis*- and *trans*-**1** were synthesized by the addition of 2

(14) *ADF2004.01*; SCM, Theoretical Chemistry, Vrije Universiteit: Amsterdam, The Netherlands, 2004. http://www.scm.com.
(15) Perdew, J. P.; Burke, K.; Ernzerhof, M. *Phys. Rev. Lett.* **1996**, *77*, 3865.
(16) Perdew, J. P.; Burke, K.; Ernzerhof, M. *Phys. Rev. Lett.* **1997**, *78*, 1396.
(17) Schreckenbach, G.; Ziegler, T. *J. Phys. Chem.* **1995**, *99*, 606.
(18) Wolff, S. K.; Ziegler, T.; van Lenthe, E.; Baerends, E. J. *J. Chem. Phys.* **1999**, *110*, 7689.
(19) Mayer, I. *Chem. Phys. Lett.* **1983**, *97*, 270.
(20) Hirshfeld, F. L. *Theor. Chim. Acta* **1977**, *44*, 129.
(21) Klamt, A.; Schuurmann, G. *J. Chem. Soc., Perkin Trans. 2* **1993**, *5*, 799.
(22) Klamt, A. *J. Phys. Chem.* **1995**, *99*, 2224.
(23) Baerends, E. J.; Branchadell, V.; Sodupe, M. *Chem. Phys. Lett.* **1997**, *265*, 481.
(24) Ziegler, T.; Rauk, A. *Theor. Chim. Acta* **1977**, *46*, 1.
(25) Ziegler, T.; Rauk, A. *Inorg. Chem.* **1979**, *18*, 1558.
(26) We were unable to perform solid-state ^{31}P NMR spectroscopy because of possible contamination of the instrument.

Table 1. Crystallographic Data for Complexes $\mathbf{1}_{trans}$, $\mathbf{1}_{cis}$, and $\mathbf{2}_{trans}$

	$\mathbf{1}_{trans}\cdot 2CH_2Cl_2$	$\mathbf{1}_{cis}\cdot 2CH_2Cl_2$	$\mathbf{2}_{trans}\cdot 2CH_2Cl_2$
formula	$C_{38}H_{72}Cl_6N_2O_2P_2U$	$C_{38}H_{72}Cl_6N_2O_2P_2U$	$C_{38}H_{70}Cl_6O_4P_2U$
M	1101.65	1101.65	1103.61
cryst syst	monoclinic	monoclinic	monoclinic
a/Å	11.575(2)	27.453(3)	43.387(7)
b/Å	12.113(2)	8.8971(9)	8.839(1)
c/Å	16.600(3)	20.764(2)	25.714(4)
α/deg	90	90	90
β/deg	90.736(3)	113.601(1)	104.301(3)
γ/deg	90	90	90
U/Å^3	2327.4(8)	4647.3(8)	9556(3)
T/K	100(2)	100(2)	100(2)
space group	$P2_1/c$	$C2/c$	$C2/c$
Z	2	4	10
μ (Mo Kα)/mm^{-1}	3.934	2.810	4.793
collected reflns	12 968	19 157	37 011
unique reflections	4745	5486	4925
R1 [$I > 2\sigma(I)$]	0.0447	0.0276	0.0516
wR2 [$I > 2\sigma(I)$]	0.1032	0.0669	0.0899

Table 2. Selected Crystallographic Bond Lengths (Å) and Angles (deg) for Complexes $\mathbf{1}_{trans}$, $\mathbf{1}_{cis}$, and $\mathbf{2}_{trans}$

	$\mathbf{1}_{trans}\cdot 2CH_2Cl_2$	$\mathbf{1}_{cis}\cdot 2CH_2Cl_2$	$\mathbf{2}_{trans}\cdot 2CH_2Cl_2$
U−O	1.792(4)	1.781(2)	1.778(5)
U−N/O	2.392(5)	2.350(2)	2.278(5)
U−Cl	2.704(2)	2.6861(7)	2.667(2)
P−N/O	1.622(5)	1.625(3)	1.535(5)
O−U−O	180.000(2)	174.24(13)	179.6(3)
Cl−U−Cl	180.0	89.75(3)	179.89(7)
N−U−N	180.000(1)	96.04(13)	
P−N/O−U	139.8(3)	140.93(15)	167.3(3)
P−N−H	112(6)	114(3)	
U−N−H	107(6)	102(3)	

equiv of Cy_3PNH to THF solutions of $UO_2Cl_2(THF)_3$ and isolation of the resultant yellow precipitate. Recrystallization of **1** from dichloromethane gave crystals with two different morphologies depending on the conditions employed.

The structure of $\mathbf{1}_{trans}$ is similar to that of *trans*-$UO_2Cl_2(Ph_3PNH)_2$ reported previously,[11] with the uranium occupying the center of a distorted octahedron (Figure 1, Tables 1 and 2). However, $\mathbf{1}_{cis}$ is somewhat unusual because all the equatorial ligand−uranium bond lengths are shorter than those in $\mathbf{1}_{trans}$. For example, the U−N bonds in $\mathbf{1}_{cis}$ are 2.350(2) Å compared with 2.392(5) Å for $\mathbf{1}_{trans}$; not as expected for a complex with greater steric interactions. These U−N bond distances are short compared with other uranyl complexes containing neutral nitrogen donors; for example, $UO_2(NO_3)_2(py)_2$ (2.543(15) Å),[27] $UO_2Cl_2(NCMe)_2(H_2O)$ (2.560(25) Å),[28] and $UO_2(NO_3)_2$(2,2′bipy) (2.578(31) Å).[29] On closer examination, it appears that the chlorides are the cause of most of the strain in the molecule. Figure 2 neatly illustrates this point. There is a significant bend of the O═U═O vector away from linearity (bond angle = 174.2(1)°) and toward the HN═PCy_3 ligands. The $HNPCy_3$ ligands are arranged with the PCy_3 groups directed above and below the equatorial plane away from the O═U═O unit and with the U(1)−N(1)−P(1) bonds (bond angle = 141.0(2)°) in the same plane as the O═U═O unit (dihedral angle O(1)−U(1)−N(1)−P(1) = 179.3(3)°). In this arrangement, the Cy_3PNH ligands appear to cause less strain in the molecule than the chlorides. These structural features may be a consequence of intermolecular forces throughout the crystal lattice. A search for hydrogen bonding revealed a weak interaction between a terminal chloride and a hydrogen of one of the CH_2Cl_2 solvent molecules (U(1)−Cl(1)···H(1S1) = 2.74 Å)[30] that may contribute to observed bond lengths and angles in $\mathbf{1}_{cis}$. No H-bonding networks were detected in $\mathbf{1}_{trans}$ or $\mathbf{2}_{trans}$.

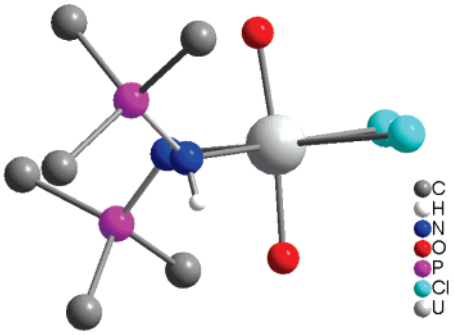

Figure 2. Ball and stick diagram of $\mathbf{1}_{cis}$ with all but the ipso carbon atoms removed for clarity.

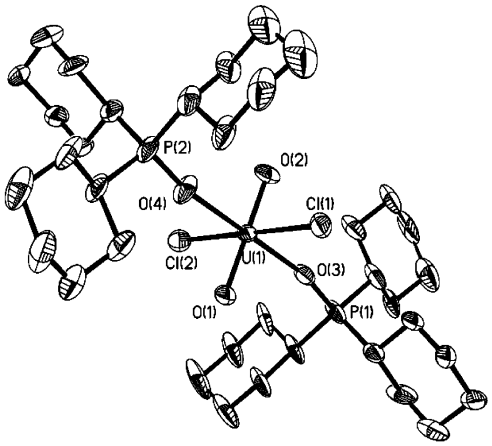

Figure 3. *ORTEP* representation of $\mathbf{2}_{trans}$.

***trans*-$UO_2Cl_2(Cy_3PO)_2$ (2).** To assist in establishing reasons behind the preference for U−HN═PR_3 vs U−O═PR_3, the phosphine oxide analogue **2** was structurally characterized (Figure 3 and Table 2). This complex was made by the simple addition of 2 equiv of Cy_3PO to $UO_2Cl_2(THF)_3$ in THF. Suitable crystals were prepared by layering hexane over a saturated solution of **2** in dichloromethane. The structure of **2** is similar in many ways to that of the phenyl analogue *trans*-$UO_2Cl_2(Ph_3PO)_2$, with comparable U−OPR_3 bonds (R = Ph, 2.300(8) Å; Cy, 2.278(5) Å).[8] The U−OPCy_3 bond length (2.278(5) Å) in **2** is considerably shorter compared with the corresponding bond of U−H*N*═PCy_3 (2.392(5) Å) in $\mathbf{1}_{trans}$; interesting, given the ligand preference illustrated in Scheme 1.

Solution Spectroscopy. As indicated by Scheme 1, we have previously shown, by ^{31}P NMR spectroscopy, that phosphinimine ligands will preferentially coordinate to $\{UO_2\}^{2+}$ (and indeed $\{NpO_2\}^{2+}$), displacing phosphine oxide

(27) Pennington, M.; Alcock, N. W.; Flanders, D. J. *Acta Crystallogr., Sect. C: Cryst. Struct. Commun.* **1988**, *44*, 1664.
(28) Hall, T. J.; Mertz, C. J.; Bachrach, S. M.; Hipple, W. G.; Rogers, R. D. *J. Crystallogr. Spectrosc. Res.* **1989**, *19*, 499.
(29) Alcock, N. W.; Flanders, D. J.; Brown, D. *Dalton Trans.* **1985**, 1001.
(30) Desiraju, G. R. *Acc. Chem. Res.* **1996**, *29*, 441.

from the uranium(VI) metal center.[11] Solution NMR spectroscopy of **1** shows two major signals in the $^{31}P\{^1H\}$ spectrum and two major signals for the N*H* protons in the ^1H NMR spectra. For both nuclei, the same ratio of relative intensities was observed (ca. 0.9/0.1). Also, variable-temperature ^1H NMR shows that each of the two signals broaden, reversibly, from 25 to 130 °C ($C_6D_4Cl_2$) (see the Supporting Information). This information is consistent with trans and cis isomers in solution that are interconverting slowly on the NMR time scale. In an attempt to establish which of the isomers is the more dominant in solution by NMR spectroscopy, we attempted to dissolve pure isomers of **1** at temperatures below 0 °C to slow the cis−trans interconversion sufficiently so that the rate of equilibrium could be established and the major isomer identified, but this was hampered by solubility problems.[26] However, solid-state Raman spectra of $\mathbf{1}_{trans}$ and $\mathbf{1}_{cis}$ show a slight difference in the O═U═O_{symm} stretch of 817 and 822 cm^{-1}, respectively (see the Supporting Information). The Raman spectrum of a solution of **1** in CD_2Cl_2 shows a O═U═O_{symm} stretch of 823 cm^{-1} (see the Supporting Information) suggesting tentative evidence for the cis isomer as the major isomer in solution, although caution must be exercised because a change from solid to solution state could also account for this small change in wavenumbers. Although only the trans isomer of **2** was isolated in the solid state, both *cis*- and *trans*-$UO_2Cl_2(Ph_3PO)_2$ have been structurally characterized,[7,8] and the ^{31}P NMR spectra of **2** exhibit two peaks at similar intensities as those observed for **1**, again indicative of cis−trans isomerization in solution.

To resolve the question of whether the cis or trans isomers of **1** and **2** dominate the solution speciation, we returned to solution ^{31}P NMR spectroscopy, this time in different solvent mixtures. It may be expected that the cis isomers would be preferentially stabilized in a solvent with a higher dielectric constant, and thus we undertook an NMR study in various ratios of $CD_2Cl_2/CDCl_3$ (ϵ = 8.93 and 4.81 for CH_2Cl_2 and $CHCl_3$, respectively). For both **1** and **2**, the major species increased in intensity on increasing $CDCl_3$ concentration, i.e., decreasing solvent dielectric constant. For pure CD_2Cl_2, the ratio of minor/major isomer is 0.12/0.88 for **1** and 0.07/0.93 for **2**, as stated previously. For pure $CDCl_3$, the ratio of minor/major isomer is 0.05/0.95 for both **1** and **2.** These results indicate that both $\mathbf{1}_{trans}$ and $\mathbf{2}_{trans}$ are the dominant species, as expected from the prevalence of trans species in the structural chemistry of $AnO_2X_2L_2$ complexes.

Finally, we previously noted the in situ formation of *cis*- and *trans*-$UO_2Cl_2(Cy_3PO)(Cy_3PNH)$ (**3**) on the addition of less than 2 mol equiv of Cy_3PNH to **2**.[11] The mixing of the equimolar ratios of **1** and **2** in CD_2Cl_2 led to the generation of a solution mixture containing **1**, **2**, and **3** in roughly 1:1:2 molar ratios (by ^{31}P NMR; see the Supporting Information). This suggests that the mixed complex is somewhat more stable than a mixture of **1** and **2**.

Clearly, the $UO_2Cl_2(Cy_3PO/Cy_3PNH)_2$ system offers an elegant route into a detailed investigation of uranyl N vs uranyl O donor bonding and cis−trans isomerization. Both studies are key to increasing our understanding of equatorial coorddination in actinyl systems. However, although experimental measurements have opened up this area of research, there is clearly a limit as to how far these results can be interpreted. We therefore turn to computational methods for a more detailed understanding of the experimental results.

Table 3. Selected Calculated Bond Lengths (Å) and Angles (deg) in the Gas Phase for Complexes $\mathbf{1}_{trans}$, $\mathbf{1}_{cis}$, $\mathbf{2}_{trans}$, $\mathbf{2}_{cis}$, $\mathbf{3}_{trans}$, and $\mathbf{3}_{cis}$[a]

	$\mathbf{1}_{trans}$	$\mathbf{1}_{cis}$	$\mathbf{2}_{trans}$	$\mathbf{2}_{cis}$	$\mathbf{3}_{trans}$	$\mathbf{3}_{cis}$
U−O_{yl}	1.811	1.819	1.803	1.807	1.808	1.813
U−N	2.441	2.470			2.431	2.483
U−O			2.393	2.432	2.400	2.422
U−Cl	2.676	2.642	2.663	2.629	2.670	2.636
P−N	1.619	1.621			1.620	1,625
P−O			1.535	1.535	1.535	1.534
O_{yl}−U−O_{yl}	177.5	170.6	178.2	174.0	177.4	172.0
Cl−U−Cl	176.7	91.1	177.2	91.0	178.3	91.5
N/O−U−N/O	175.0	91.8	177	92.1	173.9	91.7
P−N−U	145.9	144.9			147.2	143.8
P−O−U			154.7	151.4	152.8	150.6
P−N−H	111.2	110.2			111.0	110.1
U−N−H	102.0	100.6			100.8	99.8

[a] In each case, the data are the average values of two bonds.

Computational Results

Geometries. Calculated structural data for both isomers of **1** and **2** are reported in Table 3. The P−N/O bond distances are very close to the experimental values, as are those for U−Cl. The U−O_{yl} distances are slightly overestimated by the calculations but are very similar to those found recently for $[(UO_2)(OH)_2(H_2O)_2]$, i.e., another neutral uranyl complex.[31] Somewhat disappointingly, there are rather large differences between the calculated and experimental U−N and U−O distances and, for the phosphinimine systems, the experimental trend for a longer U−N distance in the cis compound is reversed computationally.[32] In agreement with experiment, calculation finds the U−O distances in the phosphine oxide to be shorter than the U−N bonds in **1**.

Among the bond angles, it is notable that there is significant reduction in the O_{yl}−U−O_{yl} angle on moving from the trans to the cis forms of both **1** and **2**. As discussed and explained above, this is also observed experimentally for **1**, for which the crystallographic angle of 174° is close to the computed angle of 171°.

The Relative Stabilities of cis and trans Isomers and of 3 vs Those of 1 and 2. The relative total bonding energies of $\mathbf{1}_{cis}$ and $\mathbf{1}_{trans}$ and $\mathbf{2}_{trans}$ and $\mathbf{2}_{trans}$, in both gas phase and CH_2Cl_2 solution, are given in Table 4. It can be seen that the relative stability of the cis and trans isomers of both compounds is significantly affected by the use of the solvent model. Thus, although the trans isomer is in both cases more stable than the cis isomer in the gas phase, the calculations

(31) Ingram, K. I. M.; Larsson Häller, L. J.; Kaltsoyannis, N. *Dalton Trans.* **2006**, 2403.

(32) We do not know why there should be such large differences between theory and experiment for just these bonds but note that our extensive previous experience suggests that the energy required to contract/elongate bonds in the vicinity of their equilibrium value is typically very small, and, hence, it may well be that forces external to the molecules in the solid state cause the U−N and U−O bonds to adopt lengths slightly different from their ideal gas-phase values. See: Kaltsoyannis, N.; Mountford, P. *J. Chem. Soc., Dalton Trans.* **1999**, 781. Menconi, G.; Kaltsoyannis, N. *Organometallics* **2005**, *24*, 1189.

Table 4. Calculated Energy Differences (kJ/mol) between the cis and trans Isomers in the Gas Phase and in CH_2Cl_2 for **1** and **2**[a]

	1	**2**
gas: $E_{cis} - E_{trans}$	24.7	15.5
CH_2Cl_2: $E_{cis} - E_{trans}$	8.8	7.1

[a] A positive energy difference means that the trans isomer is more stable.

Table 5. Calculated Dipole Moments (D) in the Gas Phase and in CH_2Cl_2 for Complexes $\mathbf{1}_{trans}$, $\mathbf{1}_{cis}$, $\mathbf{2}_{trans}$, and $\mathbf{2}_{cis}$

	$\mathbf{1}_{trans}$	$\mathbf{1}_{cis}$	$\mathbf{2}_{trans}$	$\mathbf{2}_{cis}$
gas	0.83	13.77	0.56	12.82
CH_2Cl_2	0.66	24.20	0.54	21.79

Table 6. Calculated NMR Chemical Shifts (ppm) in the Gas Phase and CH_2Cl_2 Solution and Experimental NMR Chemical Shifts for Complexes $\mathbf{1}_{trans}$, $\mathbf{1}_{cis}$, $\mathbf{2}_{trans}$, and $\mathbf{2}_{cis}$

	$\mathbf{1}_{trans}$	$\mathbf{1}_{cis}$	$\mathbf{2}_{trans}$	$\mathbf{2}_{cis}$
	calcd (gas phase)			
H (N*H*)	6.29	6.22		
P	53.6	49.8	60.7	57.9
	calcd (CH_2Cl_2 solution)			
H (N*H*)	9.95	10.9		
P	55.5	42.5	75.8	66.6
	experiment (CD_2Cl_2)			
	(major)	(minor)		
H (N*H*)	5.82	5.56		
P	58.1	58.8	73.4	73.0

in CH_2Cl_2 show a much smaller energy difference for both **1** and **2**, although the trans form is still more stable. While we cannot be certain as to the cause of the relative stabilization of the cis isomers in solution, it is most likely related to the dipole moments, as discussed above. Table 5 shows that the cis forms have much larger dipole moments in both gas phase and in solution. It is notable that the cis dipole moments increase markedly on going from gas phase to solution, whereas those of the trans isomers are small in both surroundings.

The relationship between the statistical ratio of the trans/cis isomers and the energy difference between them is given by a Boltzmann distribution

$$\frac{C_{trans}}{C_{cis}} = e^{-\Delta E/kT}$$

Here, C_{trans} and C_{cis} are the relative numbers of the trans and cis forms, ΔE is the difference in energy between the isomers, k is the Boltzmann constant, and T is the absolute temperature. The experimental (^{31}P NMR) trans/cis ratios of 0.88/0.12 for **1** and 0.93/0.07 for **2** correspond to energy differences in solution of 4.9 and 6.4 kJ/mol, respectively (at 298 K). The calculated energy differences of 8.8 kJ/mol for **1** and 7.1 kJ/mol for **2** are in good agreement with those of experiment, whereas the gas-phase calculations differ markedly from those of experiment, predicting that the trans form will massively outnumber that of the cis. It would therefore appear that the solvent has an important role to play in determining the relative abundance of the cis and trans isomers of both **1** and **2**, as indeed already observed experimentally.

As noted above, the experimental data suggest that the mixed complex $UO_2Cl_2(Cy_3PO)(Cy_3PNH)$ (**3**) is somewhat more stable than a mixture of **1** and **2**. We have probed this computationally by comparing the total bonding energy (i.e., the energy of the molecules relative to a zero in which all of the atoms are removed to infinite separation) of **3** with the average of that of **1** and **2**. In the gas phase, the average energies of **1** and **2** are 1 and 4 kJ/mol, respectively, more stable than those of **3** for the cis and trans forms. In CH_2Cl_2 solution, the average energy of the cis forms of **1** and **2** is the same as that of $\mathbf{3}_{cis}$, whereas the average energy for the trans species **3** is 3 kJ/mol more stable than the average energy of **1** and **2**. Hence, both gas phase and solvent calculations agree with the experimental observations.

Table 7. Energy Decomposition of the U−N/O Bond (kJ/mol) in the Gas Phase for Complexes $\mathbf{1}_{trans}$, $\mathbf{1}_{cis}$, $\mathbf{2}_{trans}$, $\mathbf{2}_{cis}$, and $\mathbf{3}_{trans}$[a]

	$\mathbf{1}_{trans}$	$\mathbf{1}_{cis}$	$\mathbf{2}_{trans}$	$\mathbf{2}_{cis}$	U−N in $\mathbf{3}_{trans}$	U−O in $\mathbf{3}_{trans}$
electrostatic interaction	−304.3	−299.9	−217.3	−221.8	−305.9	−222.4
Pauli repulsion	315.2	316.8	217.3	227.6	313.5	230.9
steric interaction	10.9	16.9	0.0	5.8	7.6	8.5
orbital interaction	−174.1	−174.4	−144.4	−145.7	−178.0	−146.2
total bonding energy	−163.2	−157.5	−144.4	−139.9	−170.5	−137.7

[a] The data for **1** and **2** are the average values of the two bonds.

Table 8. MBOs of the Bonds to Uranium in the Gas Phase for Complexes $\mathbf{1}_{trans}$, $\mathbf{1}_{cis}$, $\mathbf{2}_{trans}$, and $\mathbf{2}_{cis}$[a]

	$\mathbf{1}_{trans}$	$\mathbf{1}_{cis}$	$\mathbf{2}_{trans}$	$\mathbf{2}_{cis}$
$U-O_{yl}$	2.028	2.039	2.059	2.039
U−N/O	0.465	0.433	0.389	0.363
U−Cl	0.880	0.963	0.907	0.969

[a]The data are the average values for the two bonds.

NMR Chemical Shifts. Chemical shifts were calculated both in the gas phase and in CH_2Cl_2 solution and are reported in Table 6. The gas-phase N*H* chemical shifts are in good agreement with those of experiment for **1**. It is notable that $\mathbf{1}_{trans}$ has a slightly larger N*H* chemical shift than $\mathbf{1}_{cis}$, in agreement with the suggestion that the trans form is the major isomer observed experimentally. Additional calculations (data not shown), for analogues of **1** in which the Cy groups are replaced by smaller R groups such as ^{i}Pr, Me, and H, consistently produce N*H* chemical shifts that are slightly larger for the trans isomer than for the cis isomer and are comparable in value to the data shown in Table 6. Whereas the calculated gas-phase P chemical shift for $\mathbf{1}_{trans}$ is close to that of the experimental value, that for $\mathbf{1}_{cis}$ differs from experiment by ca. 6 ppm. Given the size of the target systems, discrepancies of <10 ppm are not in and of themselves discouraging, although it is disappointing that calculation predicts a reduction in the P chemical shift from $\mathbf{1}_{trans}$ to $\mathbf{1}_{cis}$, in contrast to the small increase seen experimentally. On the other hand, for **2**, calculation agrees well with experiment in finding a small reduction in the P chemical shift between the trans and the cis forms.

It might be expected that the NMR chemical shifts calculated in solution would provide a better comparison with experiment than those calculated in gas phase. However, the

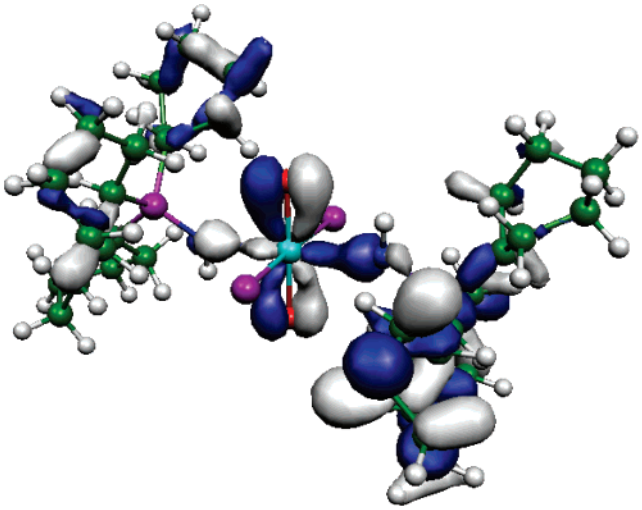

Figure 4. HOMO-22 for $\mathbf{1}_{trans}$. The contour cutoff value is 0.03.

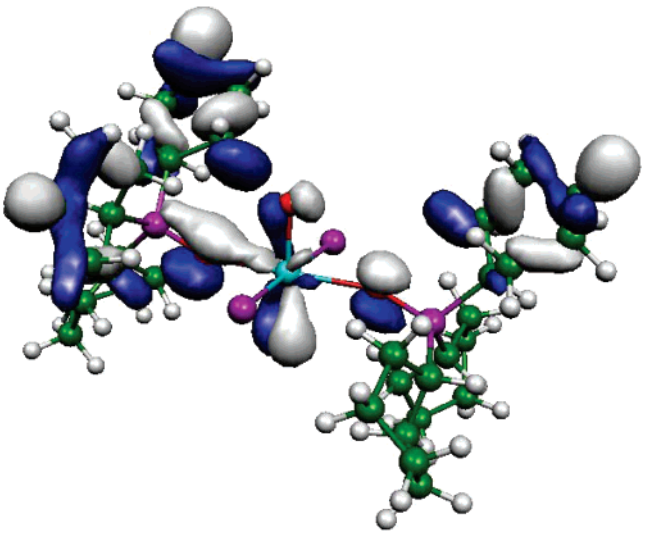

Figure 5. HOMO-28 for $\mathbf{2}_{trans}$. The contour cutoff value is 0.03.

data in Table 6 suggest that this is not the case, particularly for $\mathbf{1}_{cis}$, for which both the N*H* and P chemical shifts show the largest discrepancy from those of experiment of any of the molecules studied. Overall, we are inclined to accept the gas-phase chemical shift data as being the more reliable. It would appear that although the inclusion of solvent effects improves the calculation of the relative energies of the cis and trans forms, it makes the agreement with experimental chemical shifts rather worse.

Bond Energy Decomposition, MBOs, Molecular Orbitals, and Total Electron Densities. The ADF energy decomposition scheme was used to study the U−N/O bond in more detail, and the data are collected in Table 7. These data have been generated by breaking the molecules down into two closed-shell, neutral fragments, $UO_2Cl_2(Cy_3PNH)$ and Cy_3PNH for **1** and $UO_2Cl_2(Cy_3PO)$ and Cy_3PO for **2**. It is immediately apparent that the uranium−phosphinimine bonds are stronger than the uranium−phosphine oxide bonds, in agreement with the experimental conclusions summarized in Scheme 1. Closer analysis shows that the steric interactions are slightly larger for **1** than for **2** and also for the cis vs the

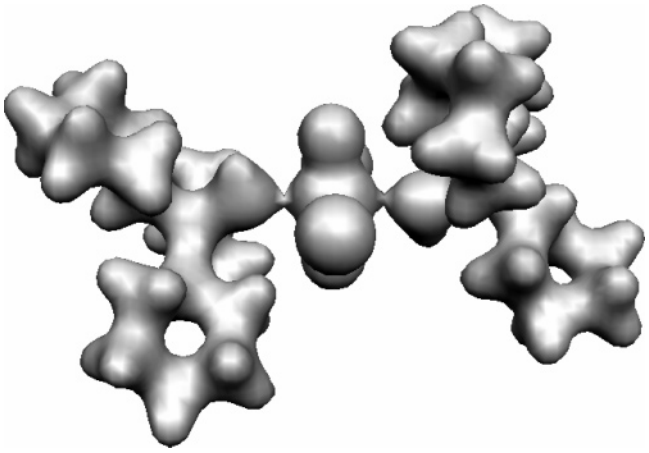

Figure 6. Total electron density for $\mathbf{1}_{trans}$. The cutoff value is 0.07.

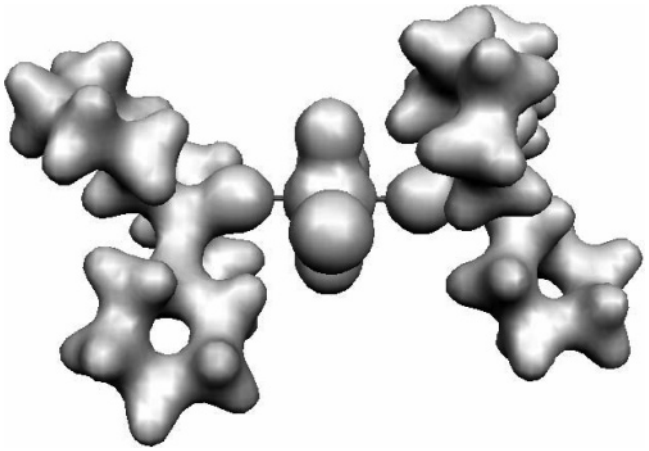

Figure 7. Total electron density for $\mathbf{2}_{trans}$. The cutoff value is 0.07.

trans compounds. In all cases, the steric term is slightly positive, and the overall negative total bonding energy results from the favorable orbital term. It is noticeable that the orbital term is significantly more negative for **1** than for **2**, and we can attribute the greater U−N bond energy to this more favorable orbital interaction.

The strengths of the U−N and U−O bonds have been probed further by studying the intermediate of $\mathbf{3}_{trans}$ seen between **1** and **2** in Scheme 1. These data are given in the final two columns of Table 7, and it can be seen that the U−N bond is once again significantly more stable than the U−O bond. Furthermore, the steric interaction is almost exactly the same in the two bonds, and, hence, the greater stability of the U−N bond clearly arises from its larger orbital interaction.

MBOs have been calculated and are presented in Table 8. The MBOs of the U−N bond in **1** are greater than the MBOs of the U−O bond in **2**, consistent with the energy decomposition analysis. MBOs of the $U-O_{yl}$ and U−Cl bonds show that they are slightly weaker in **1** compared with those of **2**. It may be tentatively concluded that the stronger U−N bonds in **1** come at the expense of weaker $U-O_{yl}$ and U−Cl interactions. This is supported, to some extent, by the Raman data, which show a lower symmetric vibrational stretching frequency for $\mathbf{1}_{trans}$ (817 cm^{-1}) compared with that of $\mathbf{2}_{trans}$ (832 cm^{-1}).

Table 9. Selected Hirshfeld Atomic and Group Charges in the Gas Phase for Complexes $\mathbf{1}_{trans}$, $\mathbf{1}_{cis}$, $\mathbf{2}_{trans}$, and $\mathbf{2}_{cis}$

	$\mathbf{1}_{trans}$	$\mathbf{1}_{cis}$	$\mathbf{2}_{trans}$	$\mathbf{2}_{cis}$
U	0.603	0.599	0.644	0.641
O (U−O_{yl})	−0.326	−0.318	−0.321	−0.314
O (U−O)			−0.256	−0.262
NH	−0.180	−0.187		
Cl	−0.263	−0.248	−0.246	−0.228

Table 3 shows that, in both **1** and **2**, the U−Cl distances in the cis forms are shorter than those in the trans forms, whereas the U−O_{yl} and U−N/O distances are somewhat longer. This is in agreement with the MBO data, which show an increase for U−Cl on going from the trans to the cis form and a concomitant decrease in the U−O_{yl} and U−N/O values. This shortening (and presumably strengthening) of the U−Cl bonds at the expense of the U−O_{yl} may be partly responsible for the bending along the O_{yl}−U−O_{yl} vector in the cis compounds, discussed earlier.

The orbital interaction term of the energy decomposition scheme cannot be straightforwardly associated with any single type of bonding interaction, as it incorporates all interactions between the chosen fragments that result from the relaxation of the starting electronic structure to self-consistency. Nevertheless, we were keen to establish the origin of the larger orbital interactions seen for the U−N bonds, and, hence, examined the molecular orbitals (MOs) of both **1** and **2**. In particular, we were interested to identify MOs with appreciable U−N and U−O σ-bonding character, as it is expected that the uranium−phosphinimine and uranium−phosphine oxide interactions are primarily σ in nature. This type of analysis can be quite difficult for large molecules without any symmetry elements, and hence we were pleased to locate HOMO-22 of $\mathbf{1}_{trans}$, shown in Figure 4, which is σ bonding between the uranium f orbital involved in the uranyl π_u level and the phosphinimine N atoms. By contrast, there is no clearly analogous orbital in $\mathbf{2}_{trans}$, the closest equivalent being HOMO-28, shown in Figure 5. It may therefore be that the larger orbital interactions seen in **1** arise from stronger U−N σ bonding than the U−O σ bonding seen in **2**.

Additional evidence for greater covalency in the phosphinimine compounds can be found from examination of the total electron density, shown for $\mathbf{1}_{trans}$ and $\mathbf{2}_{trans}$ in Figures 6 and 7, respectively. It can clearly be seen that there is a greater electron density along the U−N bonds than along the U−O bonds, reinforcing the conclusions from the energy decomposition analysis, MBOs, and examination of the molecular orbitals.

Atomic Charges. The Hirshfeld charge analysis scheme has been used to calculate atomic charges in **1** and **2**, and the results for the U atom and the atoms directly bonded to it are presented in Table 9. Comparison of **1** with **2** shows that the charges on the O_{yl} and Cl atoms are not significantly different from one another. Larger differences are seen for the U atom and for the O (phosphine oxide)/NH (phosphinimine) units. The U atom is more positive in **2** than in **1**, and the O atom is more negatively charged than the NH unit in **1**. These data suggest that the U−O bond in **2** is more ionic than the U−N bond in **1**.

Summary and Conclusions

Experimentally, it is observed that phosphinimine ligands displace phosphine oxide ligands in **2** to form **1** (Scheme 1). Our calculations are consistent with this effect in that the U−N bonds in the phosphinimine systems are found to be significantly stronger (by ca. 20 kJ mol^{-1}) than the analogous U−O bonds in the phosphine oxide compounds and that this increased bond strength is attributable to larger orbital interactions in the Ziegler−Rauk energy decomposition sense. Furthermore, analysis of the molecular orbitals reveals clearer U−N σ bonding than the σ bonding of U−O in **2**, and examination of the total electron densities reveals a greater charge buildup along the U−N vectors than along the U−O vectors. MBO data support these conclusions in finding larger U−N bond orders than those in U−O, and the smaller MBOs of the U−O_{yl} and U−Cl bonds in **1** than **2** may well be a consequence of the stronger U−N bonds in **1** compared with the U−O bonds in **2**.

Experimental solution NMR spectroscopic data show that **1** and **2** have two isomers of cis and trans conformation, which exist in ratios of 0.12/0.88 and 0.07/0.93, respectively. ^{31}P NMR experiments in CD_2Cl_2 and $CDCl_3$ indicate that in both cases the trans isomer is the dominant species. This is in agreement with the calculated energies for both **1** and **2** in the gas phase and in solution.

In summary, the comparatively small difference in the calculated energies between the cis and trans isomers of **1** and **2** have provided a rationale for the occasional observations of cis and trans isomers of the TB $[UO_2X_2L_2]$ family of complexes and predict that solvents of higher dielectric constants will tend to favor a greater proportion of the cis isomer. In addition, calculations point to the increased covalency in the U−N vs U−O interaction as the main reason for the increased stability of the uranyl phosphinimine vs uranyl phosphine oxide complexes.

Acknowledgment. The UCL team is grateful to the EPSRC for a project studentship to L.J.L.H. (Grant GR/S95169/01) and for computing resources under Grant GR/S06233/01. The CRR Manchester group is grateful to the EPSRC for a PDRA (SMC Grant GR/595152/01), EPSRC/The University of Manchester for project student funding (M.P.R.), and Nexia Solutions, Ltd., and the U.K. Nuclear Decommissioning Authority (M.J.S.).

Supporting Information Available: Three CIF files and one PDF file. This material is available free of charge via the Internet at http://pubs.acs.org.

IC062031M